

# Low-Power High-Bandwidth Non-Polar InGaN Micro-LEDs at Low Current Densities for Energy-Efficient Visible Light Communication

Shijie Zhu, Xinyi Shan<sup>ID</sup>, Pengjiang Qiu<sup>ID</sup>, Zhou Wang<sup>ID</sup>, Zexing Yuan<sup>ID</sup>, Xugao Cui,  
Guoqi Zhang<sup>ID</sup>, *Fellow, IEEE*, and Pengfei Tian<sup>ID</sup>, *Member, IEEE*

**Abstract**—Recently, the rapidly developing Internet of Things (IoT) needs to support massive connectivity with high transmission data rate, which requires IoT transmitters with high speed and low power consumption. In this work, non-polar micro-LED operating at low current density of  $10 \text{ A/cm}^2$  can still maintain a high bandwidth of 508 MHz and near-peak external quantum efficiency (EQE), making it promising for low-power, energy-efficient visible light communication (VLC) to address the challenge. At  $10 \text{ A/cm}^2$ , non-polar micro-LEDs can achieve a low power consumption and high energy efficiency, still maintaining the data rate of 0.25 Gbps. In addition, data rates of 2 Gbps and 1.1 Gbps were also successfully achieved for non-polar micro-LED operating at 320 and  $50 \text{ A/cm}^2$ , respectively, to evaluate the relationship between power consumption and achievable data rate. The capability of non-polar micro-LED that can realize low-power consumption and high bandwidth at low current density is expected to play a great role in the field of energy-efficient VLC, multi-function display and IoT in the future.

**Index Terms**—Cross-medium communication, double-sided emission, micro-LED, underwater communication.

## I. INTRODUCTION

WITH ever-growing demand for Internet of Things (IoT) applications featuring low power consumption, miniaturization and high transmission data rate, VLC with unique advantages of unlicensed spectrum, high data rate and low latency is expected to greatly promote the development of IoT [1]. To meet the requirements for miniaturized IoT applications, short-range VLC with moderate data rate and low power consumption are more suitable for system stability requirements [2].

Manuscript received 12 July 2022; revised 30 August 2022; accepted 3 September 2022. Date of publication 6 September 2022; date of current version 16 September 2022. This work was supported in part by the National Key Research and Development Program of China under Grants 2021YFE0105300, 2021YFB3601000, and 2021YFB3601003, in part by the National Natural Science Foundation of China under Grant 61974031, in part by the Science and Technology Commission of Shanghai Municipality under Grant 21511101303, and in part by the Leading-edge Technology Program of Jiangsu Natural Science Foundation under Grant BE2021008-2. (*Corresponding author: Pengfei Tian.*)

The authors are with the Institute for Electric Light Sources, School of Information Science and Technology, Academy of Engineering and Technology, Yiwu Research Institute, Fudan University, Shanghai 200433, China (e-mail: 19110860004@fudan.edu.cn; 19110720037@fudan.edu.cn; 19210720058@fudan.edu.cn; 19110720024@fudan.edu.cn; 19210860058@fudan.edu.cn; cuixugao@fudan.edu.cn; g.q.zhang@tudelft.nl; pfian@fudan.edu.cn).

Digital Object Identifier 10.1109/JPHOT.2022.3204711

Reducing the size of the transmitter, such as the fabrication of micro-LED, and making the transmitter operate at low current density, are expected to achieve orders of magnitude reductions in power consumption. For example, IBM has demonstrated a low-power, small-size InGaAs/InGaN LED that operates at ultra-low injection current and can achieve a bit rate of 1 Mbps with a power consumption of  $1 \mu\text{W}$ , enabling applications including sensor networks, optogenetics and IoT [3]. Similar device performances and applications are also expected to be realized on GaN micro-LEDs in the visible light band, as GaN micro-LEDs have proven to be a promising light source with high bandwidth and excellent performance in optical communication, display, and other fields [4], [5], [6]. However, very little research thus far has evaluated the power consumption and achievable data rate of the GaN micro-LEDs simultaneously to meet the requirements of more IoT applications.

Conventional GaN micro-LEDs based on *c*-plane sapphire often require high operating current density to produce Coulomb screening and weaken the polarization field to obtain high bandwidth [7], but with high power consumption as well as an efficiency droop. For example, a specially designed *c*-plane blue micro-LED can achieve an ultra-high  $-3 \text{ dB}$  modulation bandwidth of 1.53 GHz at a current density of  $6 \text{ kA/cm}^2$ , but only about 400 MHz at  $70 \text{ A/cm}^2$  [8]. The magnitude and direction of strain in the GaN LED structure will significantly affect the strength of the polarization field, which can be improved by the choice of GaN crystal orientation [9]. In the GaN wurtzite crystal structure, the planes perpendicular to the {0001} plane (*c*-plane) with no polarization are called non-polar planes, while the intermediate planes with reduced but not completely eliminated polarization are semi-polar planes. And the comparison for modulation bandwidth characteristics of polar, semi-polar and non-polar structure GaN LEDs was also investigated in previous study [10], further indicating that semi-polar and non-polar structures can obtain higher bandwidths at low current density due to their low polarization ratio and weak quantum confined Stark effect (QCSE). Moreover, non-polar micro-LEDs have achieved a high bandwidth of 1.5 GHz at  $1 \text{ kA/cm}^2$  and 600 MHz at a much lower current density of  $20 \text{ A/cm}^2$  [11]. Although there is a breakthrough in bandwidth for non-polar micro-LEDs, the communication performance of non-polar micro-LEDs, especially at the low current density close to the operating current

density range for micro-LED display, has not been reported. In addition, there is a trade off between the transmission data rate and power consumption of micro-LEDs, but no previous study has discussed the relationship between them.

In this paper, we have experimentally demonstrated  $40\ \mu\text{m}$  non-polar blue GaN micro-LED operating at low current density for the low-power energy-efficient VLC. The high bandwidth of 508 MHz for the device at the low current density of  $10\ \text{A}/\text{cm}^2$  benefits from the non-polar orientation with low polarization and weak QCSE. Moreover, at the low current density of  $10\ \text{A}/\text{cm}^2$  corresponding to the near-peak external quantum efficiency (EQE) region, non-polar micro-LED still maintained a data rate of 0.25 Gbps over 0.2 m with a low transmitter power consumption of 0.4 mW and high energy efficiency, indicating potential advantages of non-polar micro-LED to realize low-power energy-efficient VLC. Furthermore, data rates of 2 Gbps over 0.5 m and 1.1 Gbps over 0.2 m were also successfully achieved using orthogonal frequency division multiplexing (OFDM) for non-polar micro-LED operating at 320 and  $50\ \text{A}/\text{cm}^2$ , respectively, to evaluate the relationship between power consumption and achievable data rate. This opens up an effective path to select suitable working conditions for micro-LEDs to reduce power consumption when meeting the data rate requirements of application scenarios. In addition, this is the first time to present the communication performance of non-polar micro-LEDs, especially at an ultra-low current density of  $10\ \text{A}/\text{cm}^2$  close to the operating current density range for micro-LED display, which also demonstrates that non-polar micro-LEDs have the potential to achieve both display and high-speed communication simultaneously, providing a promising candidate to expand multi-functional applications for IoT.

## II. DEVICE FABRICATION AND CHARACTERIZATION

The proposed non-polar micro-LED was fabricated on the *m*-plane ( $\bar{1}\bar{1}00$ ) bulk GaN substrate, which mainly consists of a *n*-type GaN layer, a strained-layer superlattice (SLS) structure, a six-period InGaN/GaN multiple quantum wells (MQWs) active layer, a *p*-type GaN layer, and an indium-tin-oxide (ITO) current spreading layer from bottom to top, as shown in Fig. 1(a). The InGaN/GaN QWs have a quantum well (QW) thickness of 3 nm and a quantum barrier (QB) thickness of 10 nm. The intercalated SLS structure is expected to release the stress in the quantum wells (QWs) [12]. The device fabrication process is similar to our previous study [13]. A patterned ITO layer was formed by photolithography and wet etching. Then the epitaxial structure was etched to the *n*-GaN layer using inductively coupled plasma to form a micro-LED mesa with a diameter of  $40\ \mu\text{m}$ , which was rapidly thermal annealed at  $550\ ^\circ\text{C}$  in nitrogen atmosphere to form an ohmic contact between ITO and *p*-GaN layers. The  $\text{SiO}_2$  film was deposited as a passivation layer with patterned openings at the corresponding locations for the deposition of Ti/Au bilayer as *n* and *p* electrodes. The fabricated devices were packaged on printed circuit boards by wire bonding for optoelectronic performance characterization.

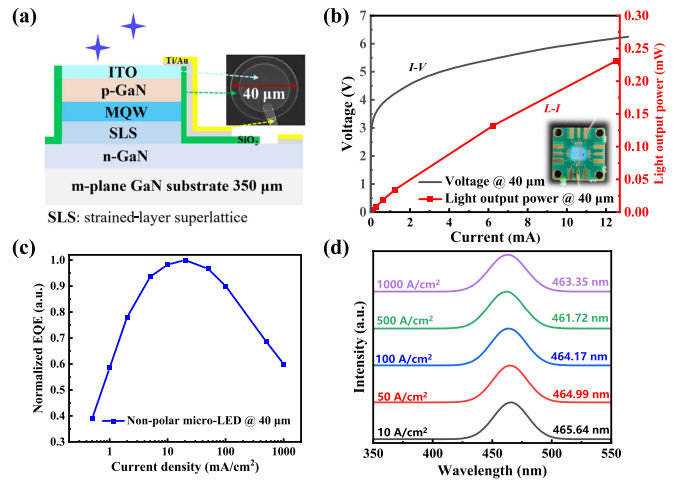


Fig. 1. (a) The schematic diagram of the non-polar micro-LED. The insert in the upper right is the plan view of the SEM micrograph for the  $40\ \mu\text{m}$  micro-LED. (b) *I-V* and *L-I* curves, (c) normalized EQE curve as a function of driving current density and (d) EL spectra at various injection current densities from  $10\ \text{A}/\text{cm}^2$  to  $1000\ \text{A}/\text{cm}^2$  of the  $40\ \mu\text{m}$  non-polar micro-LED.

The current versus voltage (*I-V*) and light output power (LOP) versus current (*L-I*) curves of the proposed  $40\ \mu\text{m}$  non-polar micro-LED are shown in Fig. 1(b). The voltages for the micro-LED operating at  $125\ \mu\text{A}$  ( $10\ \text{A}/\text{cm}^2$ ) and  $12.5\ \text{mA}$  ( $1\ \text{kA}/\text{cm}^2$ ) are  $3.3\ \text{V}$  and  $6.2\ \text{V}$ , respectively, and the corresponding power consumptions are about  $0.4\ \text{mW}$  and  $77.5\ \text{mW}$ , which means that the lower operating current can save the transmitter power consumption by orders of magnitude. The LOP of non-polar micro-LED was measured by placing the optical power meter (Thorlabs PM100D) close to the micro-LED. At a forward current of  $12.5\ \text{mA}$ ,  $40\ \mu\text{m}$  non-polar micro-LED has a LOP of  $0.23\ \text{mW}$ , and the normalized EQE curve calculated from the LOP is shown in Fig. 1(c). Non-polar micro-LED reaches peak EQE at the current density of  $20\ \text{A}/\text{cm}^2$  and has an efficiency droop at high current densities, which indicates that high luminous efficiency can be achieved at the current densities of tens of  $\text{A}/\text{cm}^2$ . And non-polar micro-LEDs have been demonstrated to have the potential to alleviate the efficiency droop problem [14]. Fig. 1(d) shows the electroluminescence (EL) spectra of non-polar micro-LED measured with the injection current densities from  $10\ \text{A}/\text{cm}^2$  to  $1000\ \text{A}/\text{cm}^2$ . The negligible wavelength shift over the large current density range is attributed to the reduction of the polarization-induced electric field, resulting in weak QCSE for non-polar micro-LEDs [15].

## III. RESULTS AND DISCUSSION

The frequency response and optical modulation bandwidth of non-polar micro-LED were measured by a vector network analyzer (VNA, PicoVNA 106), as shown in Fig. 2(a). The VNA outputs the alternating current signal, which drives the micro-LED together with the direct current (DC) through the bias-tee (Mini-Circuits ZFBT-6GW+). The emitted light is collected by the lens and received by the avalanche photodiode (APD, Hamamatsu C5658) with a  $-3\ \text{dB}$  bandwidth of 1 GHz. The received

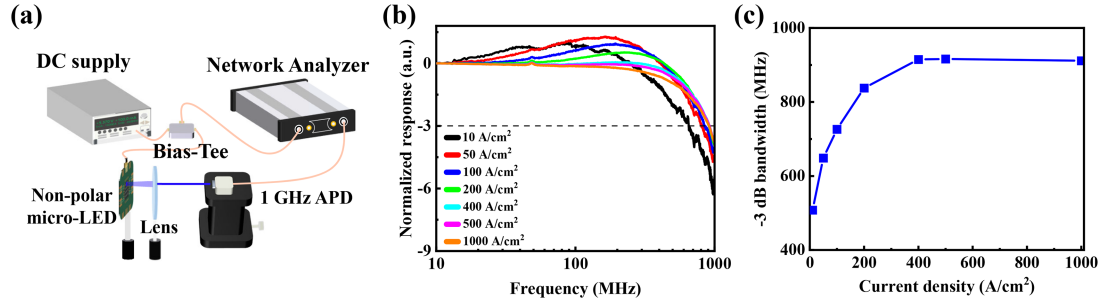


Fig. 2. Schematic diagram for the frequency response measurement system. (b) Normalized frequency responses of non-polar micro-LED at different current densities. (c) The extracted  $-3$  dB bandwidth versus current density of non-polar micro-LED.

optical signal is then converted into the electrical signal and transmitted back to the VNA for analysis to obtain the frequency response curves of the device at different current densities, as shown in Fig. 2(b). The extracted  $-3$  dB bandwidth increases with the increasing current density as shown in Fig. 2(c), due to the reduced carrier lifetime at higher injected carrier density within the QWs. A relatively high bandwidth of 911 MHz was achieved by non-polar micro-LED at  $1\text{ kA}/\text{cm}^2$  and there is an emerging trend of the saturated optical bandwidth at high current densities, which may be attributed to the limitation of the APD bandwidth. It is worth mentioning that high bandwidths of 508 and 649 MHz can be maintained at low current densities of 10 and  $50\text{ A}/\text{cm}^2$ , which may be attributed to the low polarization resulting in weak QCSE for non-polar micro-LED, consistent with the reasons for the small EL wavelength shift.

To analyze the factors affecting the bandwidth of micro-LED at low current densities, we used APSYS software to investigate the physical mechanism of high bandwidth in the aforementioned non-polar micro-LEDs [16]. The simulation structure of non-polar micro-LED was consistent with the experimental structure, and polar micro-LED on the c-plane sapphire was also set to the same structure as a control, where only the polarization conditions were different. The coefficients related to polarization electric field were set as 0 and 0.4, respectively, representing the non-polar and polar substrates. The energy band offset ratio was set as 0.7:0.3 [17], the SRH lifetime was set as 20 ns, the Auger recombination coefficient was set as  $6.8 \times 10^{-41}\text{ m}^6\text{ s}^{-1}$  [18], and the operating temperature was set as 300 K. Other parameters were set to common values, which can be found in references [17], [19]. The simulated EL spectra and normalized IQE of the  $40\text{ }\mu\text{m}$  non-polar micro-LED are shown in Fig. 3(a) and (b), which are consistent with the experimental results. The spectrum has no shift with increasing current density, while the simulated IQE has the same decreasing trend as the experimental EQE without considering the light extraction efficiency, both reaching the peak EQE near the low current density of  $10\sim20\text{ A}/\text{cm}^2$ . In addition, as can be seen from Fig. 3(b), compared with polar micro-LEDs, non-polar micro-LEDs can effectively alleviate the efficiency droop, benefiting from the absence of polarization fields. The simulated energy band diagrams of a single quantum well near the p-GaN side for polar and non-polar micro-LED at the current density of 10 and

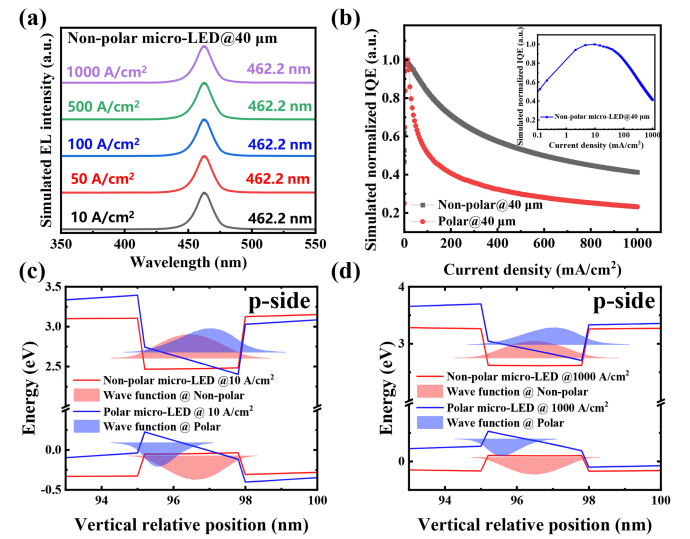


Fig. 3. (a) Simulated EL spectra at various injection current densities of the  $40\text{ }\mu\text{m}$  non-polar micro-LED. (b) Simulated normalized IQE of the  $40\text{ }\mu\text{m}$  non-polar and polar micro-LEDs. The inset is the IQE of the non-polar micro-LED with current densities in log scale. Simulated band diagrams of a single quantum well near the p-GaN side for  $40\text{ }\mu\text{m}$  non-polar and polar micro-LED at the current densities of (c)  $10\text{ A}/\text{cm}^2$  and (d)  $1000\text{ A}/\text{cm}^2$ .

$1000\text{ A}/\text{cm}^2$  are shown in Fig. 3(c) and (d). For polar micro-LED, severe band bending is observed due to the presence of the polarizing field, resulting in the formation of tilted triangular barriers and wells, which will lead to the separation of the wave functions of electrons and holes within the QWs. At the current density of  $10\text{ A}/\text{cm}^2$ , polar micro-LED has a small electron and hole wavefunction overlap value of 26.9%, thereby affecting the radiative recombination of carriers. On the contrary, the flat energy band of non-polar micro-LED results in a higher wavefunction overlap value of 55.4%, and thus can promote carrier recombination, which is the main reason for the difference in optical bandwidth. And at high current densities, such as  $1000\text{ A}/\text{cm}^2$ , the wavefunction overlap values of non-polar and polar micro-LED are 83.3% and 62%, respectively, indicating that non-polar micro-LED has higher carrier recombination rates at both high and low current densities. Therefore, non-polar micro-LED has the advantages of high bandwidth under low current density with low power consumption, which is suitable for high-speed energy-efficient VLC.

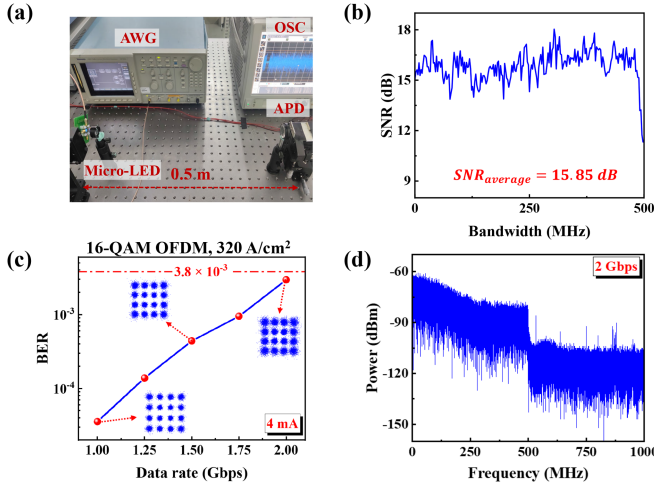


Fig. 4. (a) Experimental setup for FSO communication system. (b) SNR spectrum of the 16-QAM OFDM data with the modulation bandwidth of 500 MHz. (c) BER as a function of data rate at a transmission distance of 0.5 m. Insets are constellation diagrams of OFDM signals at different data rates. (d) Power spectrum of OFDM signals with the bandwidth of 500 MHz.

We further evaluate the communication performance of the fabricated non-polar micro-LEDs at low current densities using OFDM modulation. The experimental setup for free space optical (FSO) communication system is shown in Fig. 4(a). An arbitrary waveform generator (AWG, Tektronix AWG710B) was utilized for digital to analog conversion to output the OFDM signal, which was combined with a DC signal through a bias tee to drive the micro-LED. The modulated light from the micro-LED was collimated by the lens and transmitted in a 0.5 m free-space channel, then focused by the receiver lens into a highly-sensitive APD (Hamamatsu C12702-11) and converted into an electrical signal to the oscilloscope (OSC, Agilent DSA90604 A Infinium). The modulation and demodulation process of the OFDM data with a symbol length of 2048 and subcarrier number of 512 can refer to our previous work [20]. When using a signal bandwidth of 500 MHz, the signal-to-noise ratio (SNR) distribution of the communication system is shown in Fig. 4(b), and the average SNR is around 15.85 dB, which is sufficient for the 16-level-quadrature amplitude modulation (16-QAM) OFDM. When bit error ratio (BER) is below the forward error correction limit, the 40  $\mu$ m non-polar micro-LED can obtain the highest data rate of up to 2 Gbps at a distance of 0.5 m with the driving current of 4 mA ( $320 \text{ A}/\text{cm}^2$ ) and the peak-to-peak voltage ( $V_{PP}$ ) of 2 V, as shown in Fig. 4(c). The clarity of the constellation can be used to evaluate the signal transmission quality. And the corresponding power spectrum is exhibited in Fig. 4(d).

Then, we reduced the operating current to 625  $\mu$ A ( $50 \text{ A}/\text{cm}^2$ ), while reducing the communication distance to 0.2 m to maintain a high SNR. The achieved data rate using 4-QAM OFDM at a distance of 0.2 m was 1.1 Gbps, as shown in Fig. 5(a). Furthermore, at an extremely low current of 125  $\mu$ A ( $10 \text{ A}/\text{cm}^2$ ), we found that non-polar micro-LED can still maintain a data rate of 0.25 Gbps at a distance of 0.2 m with the  $V_{PP}$  of 0.5 V. In addition, we evaluated the transmitter power consumption versus

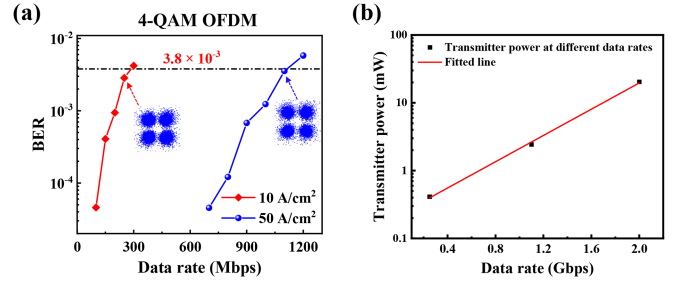


Fig. 5. (a) BER as a function of data rate for 40  $\mu$ m non-polar micro-LED operating at 50 and 10  $\text{A}/\text{cm}^2$  with a transmission distance of 0.2 m. Insets are constellation diagrams of OFDM signals corresponding to the respective achievable data rates. (b) The curve of transmitter power consumption versus the achievable data rate.

the achievable data rate curve of the VLC system based on non-polar micro-LEDs, as shown in Fig. 5(b). The transmitter power consumptions are 20.4, 2.4 and 0.4 mW for transmission data rates of 2, 1.1 and 0.25 Gbps, respectively. The high bandwidth characteristics of non-polar micro-LED at low current density can help with the low-power moderate-speed VLC systems, but there will be limitations in distance. Besides, energy efficiency (EE) is usually defined as the ratio of the achievable data rate to the total power consumption of the communication system [21]. Here we only calculated the EE of the transmitter, which are 625, 458 and 98 Gbit/Joule for non-polar micro-LED operating at the current densities of 10, 50 and  $320 \text{ A}/\text{cm}^2$ , respectively. At low operating current densities corresponding to the near-peak EQE region, the data rate decreases, but the transmitter power consumption can decrease from 20.4 mW to 0.4 mW, which results in a higher calculated EE and thus means making the transmitter more energy efficient.

#### IV. CONCLUSION

In summary, the 40  $\mu$ m non-polar blue GaN micro-LED exhibits high optical bandwidth, low power consumption and high energy efficiency at low current densities, making it promising for low-power, energy-efficient VLC system. The low polarization in non-polar orientation results in flatter QW energy bands and greater wavefunction overlap, so the device maintains a high bandwidth at low current density. At the low current density of 10  $\text{A}/\text{cm}^2$  corresponding to the near-peak EQE region, which is also close to the operating current density range for micro-LED display, non-polar micro-LED can achieve a high optical bandwidth of 508 MHz and a data rate of 0.25 Gbps over 0.2 m, demonstrating the potential to simultaneously realize micro-LED communication and display while avoiding efficiency droop. In addition, data rates of 2 Gbps over 0.5 m and 1.1 Gbps over 0.2 m were also successfully achieved for non-polar micro-LED operating at  $320$  and  $50 \text{ A}/\text{cm}^2$ , respectively, to evaluate the relationship between power consumption and achievable data rate. Combining these results, non-polar micro-LEDs are expected to realize low-power and energy-efficient communication systems, thus playing an important role in biomedical, multi-function displays, and other fields for IoT applications.

## REFERENCES

- [1] S. S. Oyewobi, K. Djouani, and A. M. Kurien, "Visible light communications for Internet of Things: Prospects and approaches, challenges, solutions and future directions," *Technologies*, vol. 10, no. 1, 2022, Art. no. 28.
- [2] B. Turan, K. A. Demir, B. Soner, and S. C. Ergen, "Visible light communications in industrial Internet of Things (IIOT)," in *The Internet of Things in the Industrial Sector*. Berlin, Germany: Springer, 2019, pp. 163–191.
- [3] N. Li et al., "Ultra-low-power sub-photon-voltage high-efficiency light-emitting diodes," *Nature Photon.*, vol. 13, no. 9, pp. 588–592, 2019.
- [4] X. Liu et al., "High-bandwidth InGaN self-powered detector arrays toward MIMO visible light communication based on micro-LED arrays," *ACS Photon.*, vol. 6, no. 12, pp. 3186–3195, 2019.
- [5] R. Lin, X. Liu, G. Zhou, Z. Qian, X. Cui, and P. Tian, "InGaN micro-LED array enabled advanced underwater wireless optical communication and underwater charging," *Adv. Opt. Mater.*, vol. 9, no. 12, 2021, Art. no. 2002211.
- [6] X. Zhou et al., "Growth, transfer printing and colour conversion techniques towards full-colour micro-LED display," *Prog. Quantum Electron.*, vol. 71, 2020, Art. no. 100263.
- [7] D. F. Feezell, J. S. Speck, S. P. DenBaars, and S. Nakamura, "Semipolar (2021) InGaN/GaN light-emitting diodes for high-efficiency solid-state lighting," *J. Display Technol.*, vol. 9, no. 4, pp. 190–198, 2013.
- [8] F. Xu et al., "C-plane blue micro-LED with 1.53 GHz bandwidth for high-speed visible light communication," *IEEE Electron Device Lett.*, vol. 43, no. 6, pp. 910–913, Jun. 2022.
- [9] M. Monavarian, A. Rashidi, and D. Feezell, "A decade of nonpolar and semipolar III-nitrides: A review of successes and challenges," *Phys. Status Solidi A*, vol. 216, no. 1, 2019, Art. no. 1800628.
- [10] M. Monavarian et al., "Impact of crystal orientation on the modulation bandwidth of InGaN/GaN light-emitting diodes," *Appl. Phys. Lett.*, vol. 112, no. 4, 2018, Art. no. 041104.
- [11] A. Rashidi, M. Monavarian, A. Aragon, A. Rishinaramangalam, and D. Feezell, "Nonpolar m-plane InGaN/GaN micro-scale light-emitting diode with 1.5 GHz modulation bandwidth," *IEEE Electron Device Lett.*, vol. 39, no. 4, pp. 520–523, Apr. 2018.
- [12] X. Yang, J. Zhang, X. Wang, C. Zheng, Z. Quan, and F. Jiang, "Enhance the efficiency of green-yellow LED by optimizing the growth condition of preparation layer," *Superlattices Microstructures*, vol. 141, 2020, Art. no. 106459.
- [13] Z. Wang, S. Zhu, X. Shan, Z. Yuan, X. Cui, and P. Tian, "Full-color micro-LED display based on a single chip with two types of InGaN/GaN MQWs," *Opt. Lett.*, vol. 46, no. 17, pp. 4358–4361, 2021.
- [14] Y. Liu, F. Feng, K. Zhang, K.-W. Chan, Z. Liu, and H. S. Kwok, "Low efficiency attenuation and stable monochromaticity for non-polar m-plane micro-light-emitting-diodes," (Micro-LEDs), in *Proc. SID Symp. Dig. Tech. Papers*, Wiley Online Library, 2022, vol. 53, no. 1, pp. 541–544.
- [15] K.-C. Kim et al., "Improved electroluminescence on nonpolar m-plane InGaN/GaN quantum wells LEDs," *Status Solidi—Rapid Res. Lett.*, vol. 1, no. 3, pp. 125–127, 2007.
- [16] Crosslight software inc. APSYS 2020 and APSYS technical manuals. [Online]. Available: <http://www.crosslight.com>
- [17] S. Lu et al., "Designs of InGaN micro-LED structure for improving quantum efficiency at low current density," *Nanoscale Res. Lett.*, vol. 16, no. 1, pp. 1–16, 2021.
- [18] R. P. Green, J. J. McKendry, D. Massoubre, E. Gu, M. D. Dawson, and A. E. Kelly, "Modulation bandwidth studies of recombination processes in blue and green InGaN quantum well micro-light-emitting diodes," *Appl. Phys. Lett.*, vol. 102, no. 9, 2013, Art. no. 091103.
- [19] I. Vurgaftman, J. á. Meyer, and L. á. Ram-Mohan, "Band parameters for III-V compound semiconductors and their alloys," *J. Appl. Phys.*, vol. 89, no. 11, pp. 5815–5875, 2001.
- [20] P. Qiu, S. Zhu, Z. Jin, X. Zhou, X. Cui, and P. Tian, "Beyond 25 Gbps optical wireless communication using wavelength division multiplexed LEDs and micro-LEDs," *Opt. Lett.*, vol. 47, no. 2, pp. 317–320, 2022.
- [21] S. Ma, T. Zhang, S. Lu, H. Li, Z. Wu, and S. Li, "Energy efficiency of SISO and MISO in visible light communication systems," *IEEE J. Light. Technol.*, vol. 36, no. 12, pp. 2499–2509, Jun. 2018.